Production of Synthesis Gas by Utilization of Municipal Solid Waste Via Dry Reforming of Methane

MUHAMMAD USMAN[1], WAN MOHD ASHRI WAN DAUD[2]

[1, 2] University of Malaya, Kuala Lumpur, Malaysia

PLEASE SCROLL DOWN FOR ARTICLE

PRODUCTION OF SYNTHESIS GAS BY UTILIZATION OF MUNICIPAL SOLID WASTE VIA DRY REFORMING OF METHANE

MUHAMMAD USMAN[1*], WAN MOHD ASHRI WAN DAUD[2]

[1, 2] University of Malaya, Kuala Lumpur, Malaysia

Abstract. This study focuses on the preparation of Ni nanoparticle and supports Ni/MgO catalysts by microemulsion assisted synthesis. The study of different synthesis parameters depicted that higher surface area and smaller Ni nanoparticles will be obtained at lower water content due to their small microemulsion droplet size. The addition of MgO support to the microemulsion system leads to a drastic reduction in particle size and provides a protective shell, as depicted by TEM analysis. XRD analysis for pure NiO, MgO, and NiO/MgO reveals the formation of a mild type of NiO-MgO solid solution formation. H2-TPR results indicate lower NiO/MgO catalysts reduction due to the lower free NiO available than pure NiO catalysts. The higher catalytic activity of supported catalysts was dedicated to its higher surface, smaller particle size, and a strong metal-support interaction than Ni nanoparticles. This study opened up avenues for scholars for further investigations in similar domains.

INTRODUCTION

The greater increase in population has led to the generation of larger amount of waste heaps and improper handling of that waste will create environmental problems [1]. It was estimated in 2012 that the rate of generation of solid waste was 1.2 kg per person per day producing 1.3 billion tonnes per year. Furthermore, it is estimated that the rate of generation of waste has been estimated to increase up to 1.42 kg person in 2025 piling up of 4.3 billion tonnes per year [2]. The conventional way of dumping municipal solid waste landfill sites leads to the generation of methane and carbon dioxide by anaerobic decomposition of organic content present in MSW [3]. Different composition of methane and carbon dioxide are generated depending on organic content weight percent, however, it is normally in the range of 40-45% methane and 55-60% carbon dioxide by volume [4]. Dry reforming of methane process draws attention of the researchers for its unique application to this landfill gas mixture and produces synthesis gas (syn-gas) [5]. Syn-gas is considered as a major building block for the synthesis of ammonia, methanol and in Fischer-Tropsch synthesis [6]. Different type of metal catalysts has been applied to dry reforming of methane process such as noble metal (Rh, Ru, Pt and Pd) and non-noble metal (Ni, Co and Fe) based catalysts [7]. Most widely studied are non-noble metal based catalysts especially Ni-based meal catalysts supported on various metal oxides due to its low cost [7]-[8]. Dry reforming of methane has not been applied on industrial scale yet due to the rapid

deactivation of catalyst induced by carbon deposition. Dry reforming of methane reaction is described by equation 1, which is described by the occurrence of three important reactions leading to the formation of syn-gas. The major reactions in the dry reforming of methane are methane decomposition (2), reverse Boudouard reaction (3) and reverse water gas shift reaction (4).

$$CH_4 + CO_2 \rightarrow H_2 + 2CO \qquad \Delta H^o_{298K} = 75{:}0 \text{ kJ/mol} \qquad (1)$$

$$CH_4 \rightarrow C + 2H_2 \qquad \Delta H^o_{298K} = 75{:}0 \text{ kJ/mol} \qquad (2)$$

$$CO_2 + C \rightarrow 2CO \qquad \Delta H^o_{298K} = 172.46 \text{ kJ/mol} \qquad (3)$$

$$CO_2 + H_2 \rightarrow CO + H_2O \qquad \Delta H^o_{298K} = 41 \text{ kJ/mol} \qquad (4)$$

It has been suggested that methane decomposition occurring on Ni metal particles leading to the production of carbon and hydrogen and CO_2 will be adsorbed on the support surface. The CO_2 adsorbed on the support surface will react with produced carbon and will regenerate the active sites and will enhance catalyst activity. Therefore, basic supports draw attention of researchers to be applied in dry reforming of methane process due to the acidic nature of CO_2. Therefore, magnesium oxide (MgO) has been selected a support material in this study [9]. In this study, microemulsion system has been selected as a synthesis method due to their various advantages such as the synthesis of metal nanoparticles at room temperature and better control over the composition of bimetallic catalyst [10]. Different parameters for the synthesis of Ni nanoparticles will be studied ranging from water to surfactant ratio, preparation time, surfactant-to-oil ratio and later on the preparation of supported Ni/MgO catalysts at the optimized synthesis parameters. The different characterization techniques such as: BET, TEM, XRD and H_2-TPR, has been appl-

*Corresponding author: Muhammad Usman
E-mail: ashri@um.edu.my

ied to study the morphology, structural behavior, reducing behavior of the pure Ni and supported Ni/MgO catalysts.

MATERIALS AND CHEMICALS

Nickel (II) nitrate hexahydrate Ni $(NO_3)_2.6H_2O$, Magnesium nitrate hexahydrate (Mg $(NO_3)_2.6H_2O$) were purchased from Acros Organics. Non-anionic surfactant Igepal CO-520 (Polyoxyethylene (5) nonylphenylether) was obtained from Sigma-Aldrich. Ammonium hydroxide (28 wt %) and ethanol was bought from R&M solutions. Different gases used in our study such as hydrogen (99.999%), methane (99.995%) carbon dioxide (99.995%) and nitrogen (99.99%) were purchased from Linde Malaysia sdn. Bhd.

Preparation of NiO Nanoparticles

Ternary phase diagram consisting of different composition of water/Igepal CO-520/cyclohexane as depicted in Table 1 were employed to prepare Ni nanoparticles. In each microemulsion system, suitable amount of cyclohexane and surfactant were added into a beaker and then left for stirring for 15 min. Later on, 2 M Ni metal solution was prepared for each sample according to water content in each system. Then, ammonium hydroxide (15 M) was added dropwise into the transparent solution to achieved pH of 11.

The microemulsion system was then sonicated for 40 min and then left for stirring for 2 h. 40 ml of ethanol was added as a destabiliser and then centrifuged for 30 min at 400 rpm. Three cycles of washing and centrifuging was done in order to remove surfactant and unreacted nickel nitrate. In the preparation of supported catalyst Ni/MgO, magnesium nitrate solution was prepared separately and then added into the microemulsion system containing Ni metal salt solution and then sonicated for 40 min. similar procedure was repeated as for Ni metal alone. The prepared sample was dried at 100 ℃ for overnight and then calcined at 450 ℃ for 2 h in air.

Characterization

The crystalline size and structure of prepared NiO and NiO/MgO before reduction was studied with X-ray diffraction (XRD) patterns by PAN analytic diffractometer. The evaluation of the diffractogram for catalysts was made by X'pert High score software. Scherrer equation was used to measure the crystalline size of Ni nanoparticles as followed

$$D_{avg} = \frac{0.9\lambda}{\beta cos\theta}\left(\frac{180}{\pi}\right)$$

Where λ denotes wavelength (0.154nm), β expresses the width of the peak at half height and Bragg angle is denoted by θ. The specific surface area, average particle size and pore size was determined by nitrogen adsorption-desorption isotherms and the study was conducted in an Autosorb BET apparatus (Micromeritics ASAP 2020). The supported catalyst structure was investigated by transmission electron microscopy (TEM) of fresh

catalysts with the assistance of FEI Tecnai™ controlled at an accelerating rate of 200 keV. To investigate the reduction behaviour and metal-support interaction of the prepared catalysts, a series of experiments were conducted by reduction with H_2. This was performed with Micromeritics TPx 2720 analyzer by placing 0.03 g of sample at the bottom of the U-shaped quartz tube. In the first step, pure He gas was passed for 60 min at 130 ℃ and flow rate of 20 ml/min. In the second step, a mixture of gas consisting of 5% H_2/N_2 was passed through the quartz tube at a flow rate of 20 ml/min and the temperature was increased from room temperature to 700 ℃ with a ramp of 10 ℃/min.

Catalytic Activity Test

The catalytic activity of the Ni and Ni/MgO catalysts were tested in fixed bed reactor by placing 0.5 g of catalysts on the catalyst bed made of quartz filter. Prior to catalytic activity test, each sample was reduced with 30% H_2/N_2 at a temperature of 550 ℃ for 2 h. After the reduction cycle was completed, the reactor was cooled down to around room temperature and then mixture of reactant gases consisting of 50% methane and 50% carbon dioxide was feed into the reactor. The outlet gases consisting of hydrogen, carbon monoxide, unreacted methane and carbon dioxide were measured with on-line gas analysers connected to the outlet of the reactor. The catalytic activity of the catalysts was measured at temperature ranging from 500 ℃ to 850 ℃ and the temperature ramp was 5 ℃/min.

RESULTS AND DISCUSSION
Effect of Surfactant, Water, Oil Composition

The synthesis of nanoparticles by microemulsion system is somewhat interesting and needs complete understanding to control the properties of nanoparticles such as surface area, particle size and crystalline size. The choice of composition of water, surfactant and oil and also the type of surfactant either cationic, anionic, non-ionic and also the type of oil such as with higher chain length or small chain length strong affects the properties. The amount of water in the microemulsion is considered to be the most important parameters the increase of water content in the system leads to the higher microemulsion droplet size and eventually larger particle size formed.

The role of surfactant in the microemulsion system is dual type, first is to act as a protective agent but also to resist the agglomeration of particles. In this study, non-ionic surfactant (Igepal Co-520) and cyclohexane was selected and their composition for each microemulsion was selected according to ternary phase diagram of water/Igepal CO-520/cyclohexane system as described in Table 1. The surface area, average particle size and crystalline size obtained by BET were also indicated in Table 1. The investigation on different microemulsion leads to the conclusion that at particular water to surfactant ratio (e.g 0.66), the sample with lower water content leads to higher surface area and smaller particle size compared to the system having higher

water content. This observation matches with the basic function of microemulsion system to exhibit smaller particle size with lower water content in a microemulsion system. This behaviour can be described by the knowledge of the influence of free and bound water over the microemuslsion structure.

The microemulsion system with lower water is considered to be bound and the micelle interface is regarded as rigid one. This situation arises as there is not sufficient amount of water to solvate polar head group of surfactant and counter ion. Therefore, the rigid nature of micelle interface leads to the lower possibility of intermicellar exchange and in turn lower growth rates [11]. On the other side, the increase in droplet size has been linked with the increase of water content leading to the liable interface and enhancing the micellar exchange process producing larger particle size [12]. Similar type of results was produced by various studied that the increase of water content leads to the increase of particle size [13], [14] and [15].

BET

Another important parameter in the synthesis of nanocatalysts is having porous structure to allow reactant to adsorb on active sites and then after reaction products are desorb from active sites. The investigation on the porous nature of NiO nanoparticle and NiO/MgO catalysts prepared was investigated by N_2 adsorption-desorption measurements. The results obtained from this analysis for pure NiO prepared by microemulsion system and also supported NiO/MgO catalyst were listed in Table 1 and Table 2, respectively. The higher surface area and smaller particle size for supported catalyst indicates the excellent ability of MgO coating to resist agglomeration of NiO nanoparticles. N_2 adsorption-desorption isotherm and pore width distribution for pure NiO is exhibited in Fig 1. The smaller BET pore size was observed for supported catalyst.

TABLE 1
SURFACE AREA AND CRYSTALLITE SIZE FOR DIFFERENT MICROEMULSION SYSTEM

Sample	ME	S/W	S/O	Single point SA[a]	BET SA[a]	BET pore size[b]	Average particle size[b]	XRD crystallite size[b]
A1	12/18/70	1.5	0.257	5.081	5.19	30.34	577.91	39.09
A2	6/9/85	1.5	0.105	23.611	23.87	20.36	125.66	27.58
A3	7/21/72	3.0	0.291	3.5588	3.65	39.62	821.20	31.36
A4	4/12/84	3.0	0.142	9.8164	9.97	37.39	300.73	24.55

a: m^2/g, b: nm

TABLE 2
SURFACE AREA AND CRYSTALLITE SIZE FOR PURE NIO AND NIO/MGO CATALYSTS

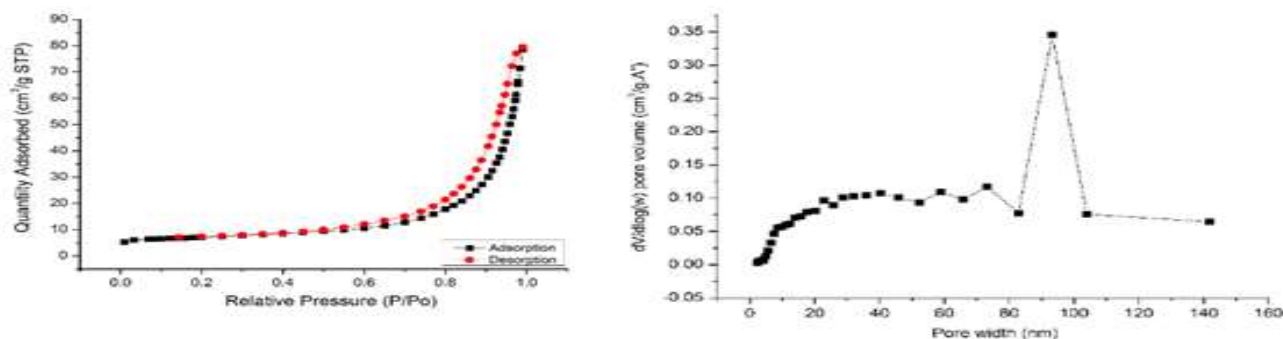| Sample	Single point SA[a]	BET SA	BET pore size[b]	Average particle size[b]	XRD crystallite size[b]
NiO	23.611	23.87	20.36	125.66	27.58
NiO/MgO	148.08	153.22	10.26	19.57	18.81

a: m^2/g, b: nm

Fig. 1. N_2-Adsorption-desoprtion isotherm and pore width distribution of sample A2.

Effect of Preparation Time

The study of kinetics of the nanoparticle synthesis is also important in the microemulsion system as it will have a significant influence over surface area and particle size. In this study, the microemulsion system for the preparation of Ni nanoparticles different preparation times (0.5, 2, 8 and 24 h) were studies for their influence on surface area. The influence of preparation time over surface area and crystallite size has been described in Table 3 and Fig 2. [16] investigated the influence of different aging time (1.5, 3, 6, 24) for the preparation of Ni@SiO$_2$ and reported better morphology with narrow size distribution and have better cavity length distribution at base case for 3h. The further increase in aging time lead to the increase in the cavity length formation and produce longer nanotube instead of more organize spherical shapes. An investigation on the influence of preparation time over the synthesis of SiO$_2$ nanoparticle via microemulsion system reveals that with the increase of aging time there was seen an increase in SiO$_2$ particle size [17]. Therefore, in our study aging time of 2 h for chosen as a base case for the preparation of Ni nanoparticles.
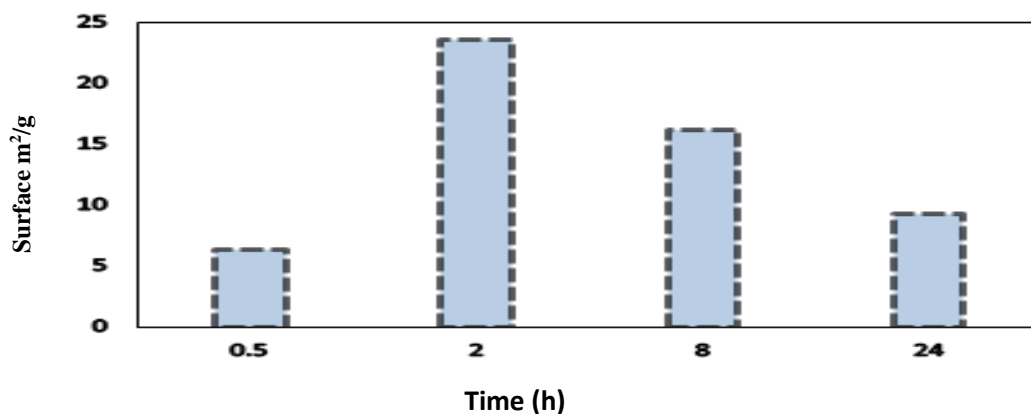

Fig. 2. Effect on surface area with respect to different preparation times

TABLE 3
EFFECT OF PREPARATION TIME ON SURFACE AREA AND CRYSTALLITE SIZE

ME	W/S	S/O	Prep. time[a]	Single point SA[b]	BET SA[b]	BET pore size[c]	Average particle size[c]	XRD crystallite size[c]
6/9/85	0.66	0.105	0.5	6.11	6.35	61.07	471.88	26.27
6/9/85	0.66	0.105	2	23.611	23.8722	20.36	125.66	27.58
6/9/85	0.66	0.105	8	16.21	16.37	25.39	183.18	25.51
6/9/85	0.66	0.105	24	9.32	9.56	34.76	313.67	31.62

a: h, b: m^2/g, c: nm

XRD Analysis

The XRD patents for calcined NiO nanoparticle prepared by microemulsion system to investigate the influence of water to surfactant ratio are exhibited in Fig 3. The XRD patters for all the NiO nanoparticle matched with the standard card of cubic NiO having JCPDS no. 01-073-1519. The 2θ values of NiO are exhibited in Fig 3a along with their corresponding crystallit phase of (111), (200), (220), (311), and (222). Fig 3b exhibits the crystalline structure of Pure NiO, Pure MgO and supported NiO/MgO catalysts with their corresponding 2θ peaks. The formation of NiO-MgO solid solution has been evident by looking at higher 2θ values of 62.37°, 75.52° and 78.83°. This arises due to the addition of MgO to NiO and shifting of the peaks to slightly lower values and are quite similar to the structure of NiO and MgO [18, 19].
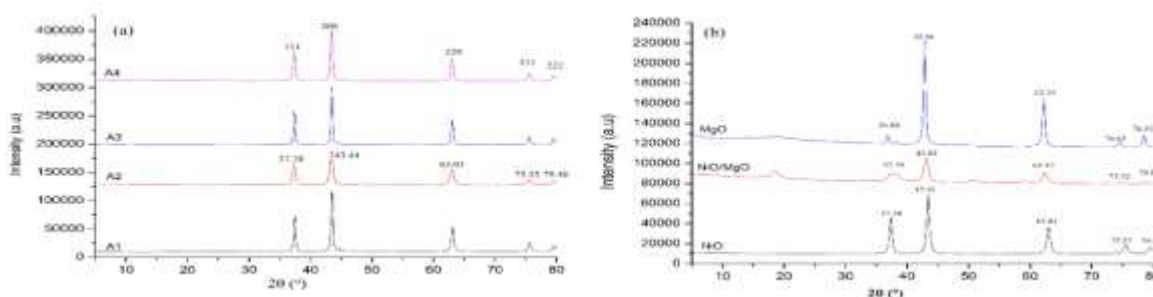

Fig. 3. A) XRD patterns for different water to surfactant ratios, b) xrd patterns for nio, mgo and ni/mgo.

TEM Analysis

TEM images depicts the morphology and structural characteristics of Ni/MgO catalysts. TEM images exhibited that the addition of coating material (MgO) leads to the better nanoparticle distribution and also restricts the agglomeration of Ni nanoparticles (Fig 4). This leads to higher surface area and smaller particle size for supported Ni/MgO catalysts as also evident in BET results.
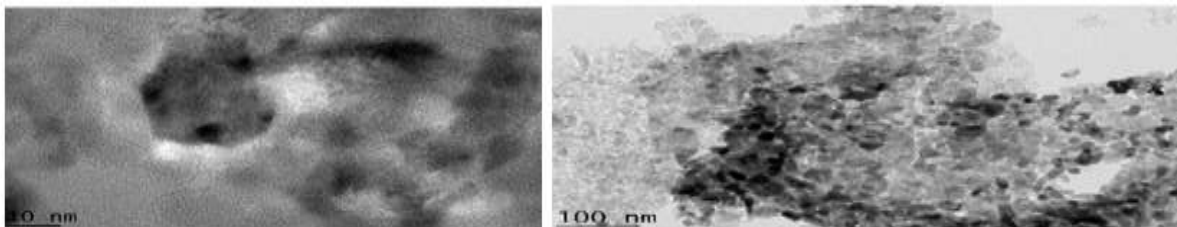

Fig. 4. TEM images of ni/mgo catalysts

H₂-Temperature Programme Reduction (TPR)

H$_2$-TPR experiments are conducted to investigate the reduction behaviour of NiO and NiO/MgO catalyst. The reduction behaviour will also indicate the metal-support interaction and also the formation of NiO-MgO solid solution. The reduction of NiO/MgO catalysts indicates the presence of partially NiO-MgO solid solution and the presence of free NiO which are not having strong metal-support interaction. The lower consumption of H$_2$ of NiO/MgO compared to NiO in Table 4 indicates that most of NiO has been in strong interaction with MgO however still there is free NiO present in the NiO/MgO [18]. The reduction peak temperatures are exhibited in Fig 5.

TABLE 4
REDUCTION PEAK TEMPERATURES AND H$_2$ CONSUMPTION FOR UNSUPPORTED AND SUPPORTED CATALYST

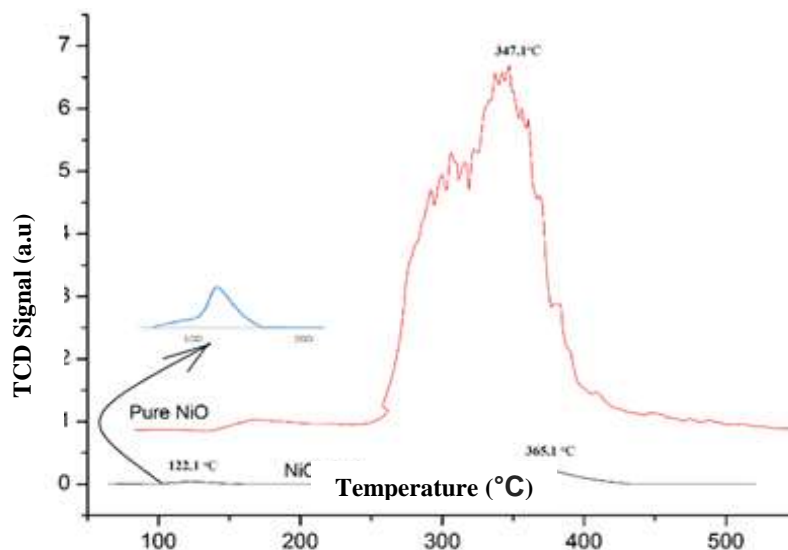| Samples	Peak Temperature (°C)		H$_2$ Consumption (ml/g STP)
	TL	TM	
NiO	-	347.2	288.88
NiO/MgO	122.1	365.1	29.92

Fig. 5. H$_2$-tpr profiles for nio and nio/mgo catalyst.

Activity Test

The catalytic activity of Ni and Ni/MgO catalysts at different temperature are indicated in Fig 6. Ni/MgO exhibited higher methane and carbon dioxide conversion compared to Ni nanoparticles. Dry reforming of methane reaction (eq 1) has been suggested to have series of reactions which are described earlier such as methane decomposition (eq 2), reverse Boudouard reaction (eq 3) and RWGS (eq 4). Methane decomposition reaction leads to the production of carbon and H$_2$ on Ni particles

and the CO$_2$ adsorbed on basic active sites reacts with produced C to form CO. Therefore, for dry reforming reaction basic supports are considered to be important to enhance more CO$_2$ chemisorption and leads to lower carbon deposition [20]. The reason that higher CO$_2$ conversion was observed for both Ni and Ni/MgO catalyst can be ascribed to the occurrence of RWGS, in this reaction CO$_2$ utilizes also the produced hydrogen and produced more CO. therefore, higher CO$_2$ conversion were observed for both catalyst and it was evident also by the presence of traceable amounts of water in the outlet of the reactor [9].
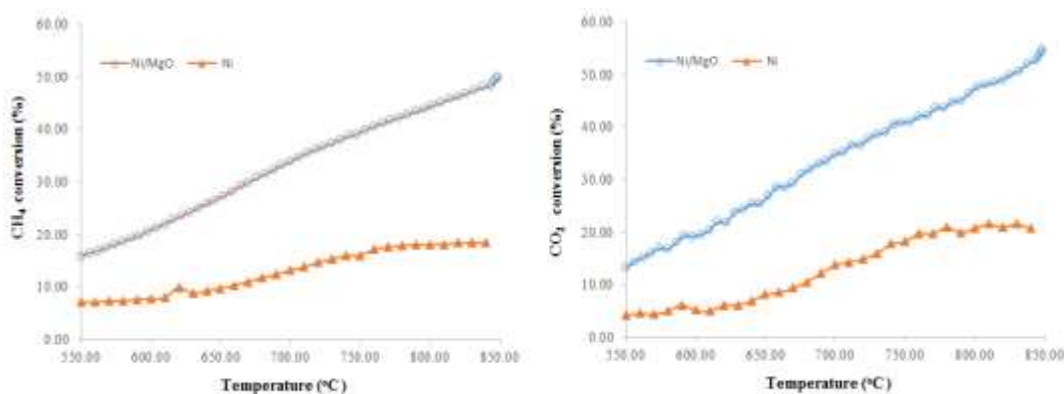

Fig. 6. Methane and carbon dioxide conversions for ni and ni/mgo catalyst.

CONCLUSION AND RECOMMENDATIONS

The preparation of Ni nanoparticles by microemulsion system leads to the conclusion that lower water content at constant water to surfactant ratio is very suitable to produce higher surface area and smaller particle size. Furthermore, the coating of Ni nanoparticle with basic metal oxide (MgO) enhanced crystallinity of the Ni/MgO catalysts. The higher methane and CO$_2$ conversion are dedicated to the higher surface area, small particle size and

lower agglomeration of Ni particles in supported catalysts. However, further studies are underway to investigated stability, testing different composition of Ni and MgO, and analysing basicity of active site by CO_2 adsorption experiments.

Declaration of Conflicting Interests

It is hereby declared that this study has no conflicts of interest.

REFERENCES

[1]   Z. Z. Noor, R. O. Yusuf, A. H. Abba, M. A. Abu Hassan and M. F. Mohd Din, "An overview for energy recovery from municipal solid wastes (MSW) in Malaysia scenario," *Renewable and Sustainable Energy Reviews,* vol. 20, pp. 378-384, 2013.

[2]   D. Hoornweg and P. Bhada-Tata, "What a waste: A global review of solid waste management," Washington DC: World Bank, 2012.

[3]   M. F Abushammala, N. E. A Basri, H. Basri, A. H. El-Shafie and A. A. H. Kadhum, "Regional landfills methane emission inventory in Malaysia," *Waste Management & Research,* vol. 29, no. 8, pp. 863-873, 2011.

[4]   B. Raco, R. Battaglini and M. Lelli, "Gas emission into the atmosphere from controlled landfills: An example from Legoli landfill (Tuscany, Italy)," *Environmental Science and Pollution Research*, vol. 17, no. 6, pp. 1197-1206, 2010.

[5]   M. C. J. Bradford and M. A. Vannice, "CO_2 reforming of CH_4," *Catalysis Reviews,* vol. 41, no. 1, pp. 1-42, 1999.

[6]   S. T. Oyama, P. Hacarlioglu, Y. Gu and D. Lee, "Dry reforming of methane has no future for hydrogen production: Comparison with steam reforming at high pressure in standard and membrane reactors. *International Journal of Hydrogen Energy,* vol. 37, no. 13, pp. 10444-10450, 2012.

[7]   D. Liu, X. Y. Quek, W. N. E. Cheo, R. Lau, A. Borgna and Y. Yang, "MCM-41 supported nickel-based bimetallic catalysts with superior stability during carbon dioxide reforming of methane: Effect of strong metal–support interaction," *Journal of Catalysis,* vol. 266, no. 2, pp. 380-390, 2009.

[8]   Y. J. O. Asencios and E. M. Assaf, "Combination of dry reforming and partial oxidation of methane on NiO–MgO–ZrO_2 catalyst: Effect of nickel content," *Fuel Processing Technology,* vol. 106, pp. 247-252, 2013.

[9]   R. Zanganeh, M. Rezaei and A. Zamaniyan, "Dry reforming of methane to synthesis gas on NiO–MgO nanocrystalline solid solution catalysts," *International Journal of Hydrogen Energy,* vol. 38, no. 7, pp. 3012-3018, 2013.

[10] M. Boutonnet, S. Lögdberg and E. Elm Svensson, "Recent developments in the application of nanoparticles prepared from w/o microemulsions in heterogeneous catalysis," *Current Opinion in Colloid & Interface Science,* vol. 13, no. 4, pp. 270-286, 2008.

[11] J. Eastoe, M. J. Hollamby and L. Hudson, "Recent advances in nanoparticle synthesis with reversed micelles," *Advances in Colloid and Interface Science*, vol. 128, no. 130, pp. 5-15, 2006.

[12] M. A. López-Quintela, C. Tojo, M. Blanco, L. G. Rio and J. Leis, "Microemulsion dynamics and reactions in microemulsions," *Current Opinion in Colloid & Interface Science,* vol. 9, no. 3, pp. 264-278, 2004.

[13]   J. Chandradass and D. S. Bae, "Synthesis and characterization of alumina nanoparticles by igepal CO-520 stabilized reverse micelle and sol-gel processing," *Materials and Manufacturing Processes,* vol. 23, no. 5, pp. 494-498, 2008.

[14]   J. Chandradass and K. H. Kim, "Size-controlled synthesis of $LaAlO_3$ by reverse micelle method: Investigation of the effect of water-to-surfactant ratio on the particle size," *Journal of Crystal Growth,* vol. 311, no. 14, pp. 3631-3635, 2009.

[15] J. Chandradass, M. Balasubramanian, D. S. Bae, J. Kim and K. H. Kim, "Effect of water to surfactant ratio (R) on the particle size of $MgAl_2O_4$ nanoparticle prepared via reverse micelle process," *Journal of Alloys and Compounds*, vol. 491, no. 1, pp. L25-L28, 2010.

[16] K. A. Dahlberg and J. W. Schwank, "Synthesis of Ni@SiO_2 Nanotube Particles in a Water-in-Oil Microemulsion Template," *Chemistry of Materials,* vol. 24, no. 14, pp. 2635-2644, 2012.

[17]   Lin. M, "Synthesis of magnetic nanoparticles and nanocomposites via water-in-oil microemulsions," Ph.D. dissertation, Loughborough Univ., Loughborough, UK, 2006. Available: https://dspace.lboro.ac.uk/2134/7817

[18]   Y. J Asencios, J. D. Bellido and E. M. Assaf, "Synthesis of NiO–MgO–ZrO_2 catalysts and their performance in reforming of model biogas," *Applied Catalysis A: General,* vol. 397, no. 1, pp. 138-144, 2011.

[19] J. Feng, Y. Ding, Y. Guo, X. Li and W. Li, "Calcination temperature effect on the adsorption and hydrogenated dissociation of CO_2 over the NiO/MgO catalyst," *Fuel*, vol. 109, pp. 110-115, 2012.

[20] F. Meshkani and M. Rezaei, "Nickel catalyst supported on magnesium oxide with high surface area and plate-like shape: A highly stable and active catalyst in methane reforming with carbon dioxide," *Catalysis Communications,* vol. 12, no. 11, pp. 1046-1050, 2011.